FA9550-10-0177 (STTR Phase II, Dr. Gernot Pomrenke)
9/30/2010 TO 9/29/2011

Frequency Agile THz Detectors for Multiplicative Mixing

Final Progress Report
September 29, 2011

Dr. Sangwoo Kim

Technical Representative

(626) 471-9762

20111027019

REPORT DOCUMENTATION PAGE

1. REPORT DATE	2. REPORT TYPE	3. DATES COVERED
Sept. 29, 2011	FINAL PROGRESS REPORT	Sept. 30, 2010 to Sept. 29, 2011

4. TITLE AND SUBTITLE

FREQUENCY AGILE THZ DETECTORS FOR MULTIPLICATIVE MIXING

5a. CONTRACT NUMBER

FA9550-10-C-0177

5b. GRANT NUMBER

5c. PROGRAM ELEMENT NUMBER

6. AUTHOR(S)

Dr. Sangwoo Kim, Principal Investigator

5d. PROJECT NUMBER

5e. TASK NUMBER

5f. WORK UNIT NUMBER

7. PERFORMING ORGANIZATION NAME(S) AND ADDRESS(ES)

Tanner Research, Inc.
825 South Myrtle Avenue
Monrovia, CA 91016-3424

8. PERFORMING ORGANIZATION REPORT NUMBER

9. SPONSORING/MONITORING AGENCY NAME(S) AND ADDRESS(ES)

USAF, AFRL
AF OFFICE OF SCIENTIFIC RESEARCH
875 N. RANDOLPH ST. ROOM 3112
ARLINGTON, VA 22203

10. SPONSOR/MONITOR'S ACRONYM(S)

11. SPONSOR/MONITOR'S REPORT NUMBER(S)

12. DISTRIBUTION/AVAILABILITY STATEMENT

Distribution Statement A: Approved for public release; distribution is unlimited.

13. SUPPLEMENTARY NOTES

None

14. ABSTRACT

A novel FET-based terahertz multiplicative mixer was demonstrated with a terahertz homodyne mixer system. The first fabricated devices operated at 370 GHz and achieved NEPmix (mixer noise equivalent power) of 1 nW/Hz with PLO (local oscillator power) of 8 W. After design revisions, the operating frequency of the second generation devices was raised to 570 GHz (NEPmix = 26.4 nW/Hz with PLO = 1.5 W). The measured performance metrics (NEP and PLO) are consistent with our long term goal of building an imager array with a single quasi-optically coupled mW-level LO source.

15. SUBJECT TERMS

Terahertz, field-effect-transistor, multiplicative mixer, homodyne detection, imaging arrays, quasi-optical and standoff terahertz imaging

16. SECURITY CLASSIFICATION OF:			17. LIMITATION OF ABSTRACT	18. NUMBER OF PAGES	19a. NAME OF RESPONSIBLE PERSON
a. REPORT	b. ABSTRACT	c. THIS PAGE	Same as report	12	Kevin Dinniene, Controller
Unclassified	Unclassified	Unclassified			**19b. TELEPHONE NUMBER** (626) 471-9778

Standard Form 298
Prescribed by ANSI Std. Z39.18

1   Overview

During part one of this modified Phase II STTR effort, we demonstrated a novel FET-based terahertz multiplicative mixer by constructing a terahertz homodyne mixer system with the new mixer component. The first fabricated devices operated at 370 GHz (NEP_{mix} = 1 nW/Hz @ P_{LO} = 8 µW, see Sections 4.1~4.4). After design revisions, the operating frequency of the second generation devices was raised to 570 GHz (NEP_{mix} = 26.4 nW/Hz @ P_{LO} = 1.5 µW, see Section 4.5). The measured performance metrics (NEP and P_{LO}) are consistent with our long term goal of building an imager array with a single quasioptically coupled mW-level LO source (see end of Section 4.4). We are in search of additional funding so that part two of the SOW may be executed to develop imaging arrays.

2   Overall goal of the proposed effort

The overall goal of the proposed effort is to design and build a high-sensitivity mixer detector that can provide for standoff (>10 m), real-time monitoring of concealed weapons. Thus, the end goal is a **FET multiplicative mixer** (Figure 1, right) that can detect terahertz radiation more efficiently than the existing SOA technologies (Figure 1, left) by removing significant loss and noise sources terms inherent in the current SOA mixing detectors (red box in Figure 1, left).
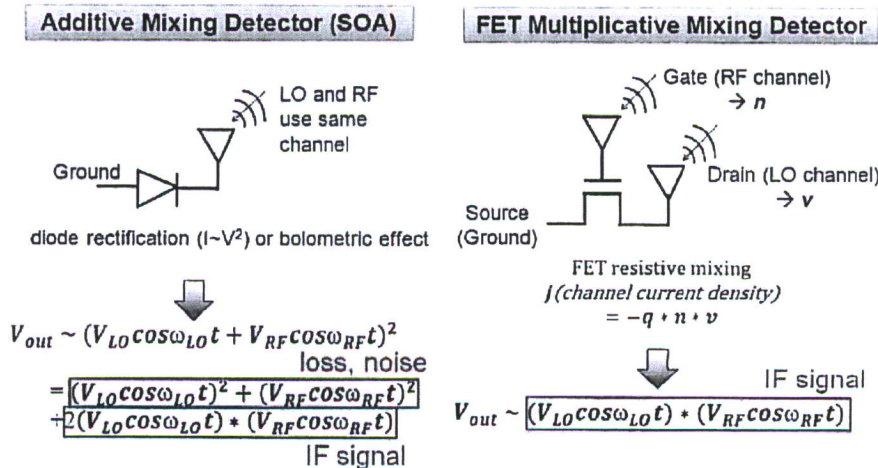

Figure 1: (Left) Schematic of SOA additive type mixers (e.g., diode mixers and bolometer mixers), (right) schematic of multiplicative type mixers using FETs. Additive mixers have loss and noise terms in the mixing scheme (red box on the left), whereas multiplicative mixers generate only the necessary IF signal (blue boxes). Therefore, the proposed FET multiplicative mixers can achieve better performance than additive mixers.

Our phase I work demonstrated FET based self-mixing *direct* detectors. The results from the phase I effort strongly suggested that a new type of efficient mixer (i.e., FET multiplicative mixer) could be developed. Although already very common in the RF frequency regime, FET multiplicative mixers had not been demonstrated at THz frequencies. Therefore, our project goal for this modified Phase II was to demonstrate the proof of concept for FET multiplicative mixers. This goal was achieved.

3 Schedule Performance

This modified Phase II STTR project was awarded $100,000 for a 1-year period. Accordingly, we set our **modified project goal (milestone to achieve) as the proof of concept demonstration of the multiplicative mixer design**. This goal was achieved early in the effort, with the first generation of devices, which were functional at 370 GHz (see Figure 2). For the remainder of the project period, in an effort to improve the performance of the novel mixers, a revised photomask was developed and a second generation of devices was fabricated. These additional tasks were also finished within the Phase II schedule. As a result, the operating frequency of the multiplicative mixers has been demonstrated up to 570 GHz (see also Figure 2).

The results are being published as two journal papers. The first, an experimental paper [1], has been submitted to Applied Physics Letters (recently turned down. We will submit it to another journal). The second, a theory paper [2], has been submitted to the Journal of Applied Physics.

The second part of the original SOW was not funded within the current contract. We are currently looking for additional funding for continuation of this effort to optimize the detector design and build and demonstrate a 2x2 array of detector elements (Figure 2).
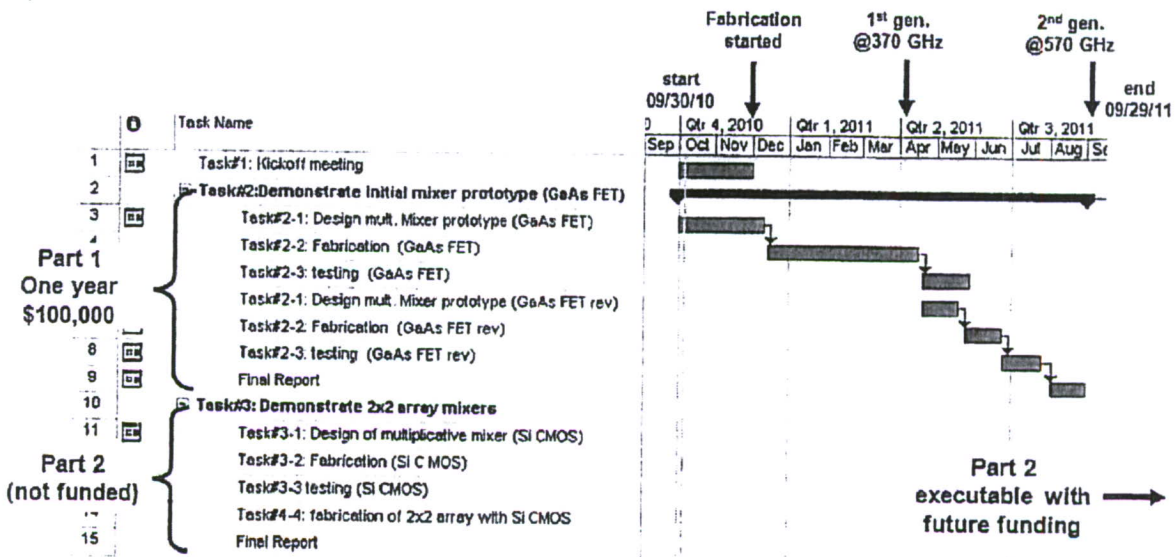

Figure 2: Schedule performance of this modified phase II STTR project. Two cycles of design-fabrication-testing were finished according to schedule, yielding proof of concept demonstration at 370 GHz and an extension of the operating frequency up to 570 GHz.

4 Summary of achieved specific goals

In order to achieve the overall goal (Section 2) of this project, we set specific task/milestones for the modified Phase II effort, those being the design (Section 4.1), the fabrication (Section 4.2), and the testing (Section 4.3) of the multiplicative mixing detector. All of these initial specific goals were achieved by early April. Therefore, we set additional goals for the remainder of the time, to design, fabricate, and test a second generation device to provide improved performance and extend the operating frequency of the devices (Section 4.5). In our previous telephone conference and an interim report,

we described the results of our initial study, which demonstrated the proof of concept of the multiplicative mixer device. We also laid out a roadmap to reach the end goal of an "improved SNR" device in the near future, as well as the long term goal of a THz imaging array. In this final progress report, we will briefly summarize the specific milestones achieved with our first fabricated devices and will summarize the additional achievement of the second generation of devices.

4.1 Design

During the first two months of this project, antennas and filters were designed using commercial finite element method software (COMSOL) (Figure 3). Initially, the antennas were designed for an operation at 670 GHz. However, the first fabricated mixers were found not to have sufficient response at this target frequency (We think it is due to poor impedance matching and low input THz power). To achieve noticeable detector response, we moved the test frequency down to 300~400 GHz, where more radiative power is available from our THz sources, and the existing antenna-filter structure is resonant at two-fold the wavelength (Figure 3). Consequently, we obtained all of our experimental results from the first generation of devices at the lower frequency (300~400 GHz) band.
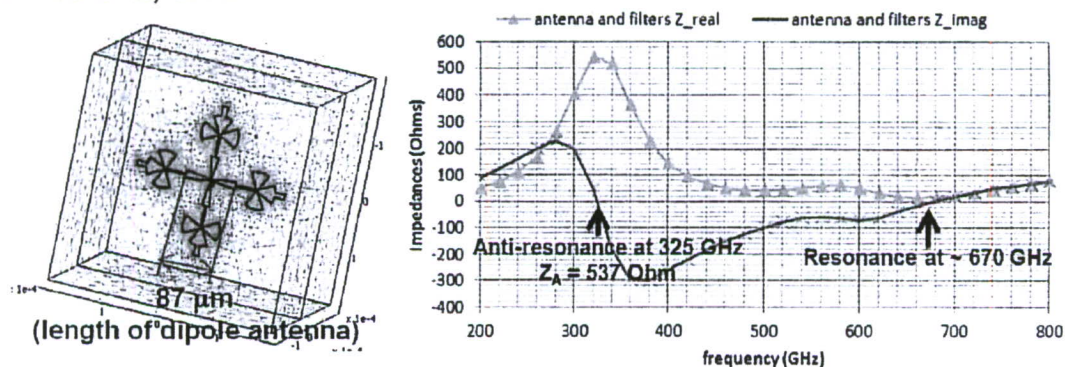

Figure 3: (Left) simulated 3D model of a dipole antenna and IF filters, (right) simulated antenna impedances vs. frequency exhibiting resonances at 325 GHz (anti-resonance) and at 670 GHz (resonance). The green curve is the real part and the violet curve is the imaginary part of the impedances. COMSOL (finite element method simulation software) was used for this study.
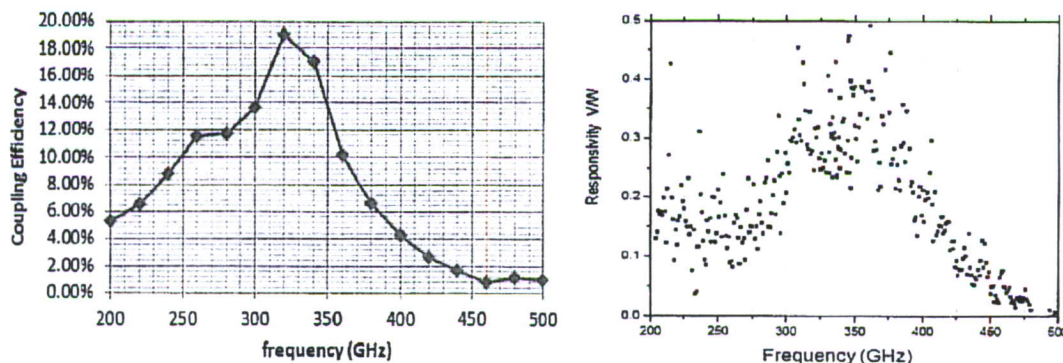

Figure 4: (Left) simulated (with COMSOL) antenna coupling efficiency vs. frequency, (right) measured direct-detection responsivity vs. frequency (note: responsivity scale has been corrected since the last report).

Our simulation studies indicated the antenna-filter structure were at resonance (anti-resonance in Figure 3, right) at 325 GHz. The predicted resonance peak (Figure 4 left) matched well with the measured direct detector responsivity (Figure 4 right), except for a slight frequency shift.

4.1.1 Theory of FET multiplicative mixing

In this subsection, we will describe the theory of FET multiplicative mixing. More elaborate discussion can be found from our theory paper [2].

The rectification of high frequency currents in transistors occurs due to local simultaneous variation of the carrier density and carrier velocity by the THz bias (see Figure 5).
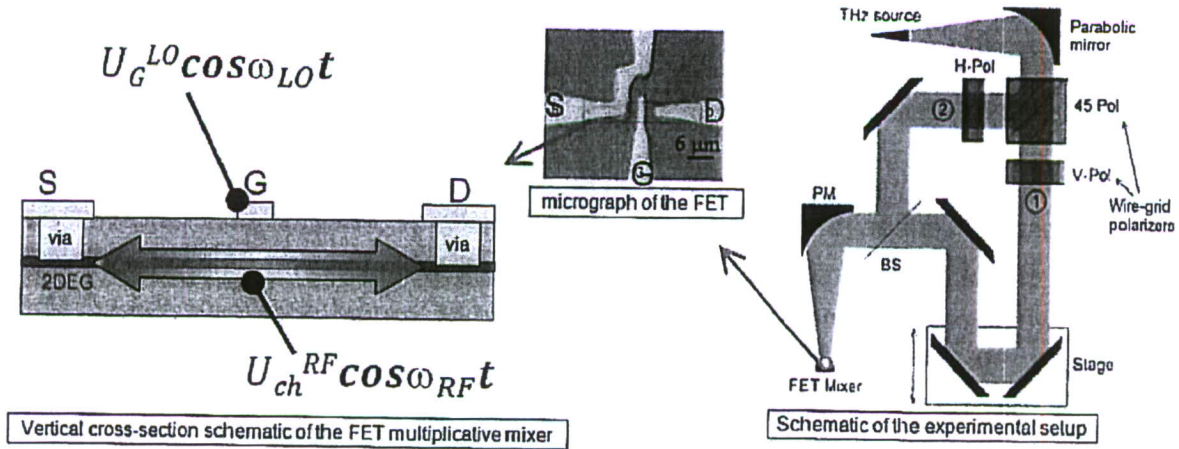

Figure 5: Schematic of homodyne detection system based on the FET multiplicative mixer. The output of a single THz source was split into two orthogonally polarized beams to simulate the LO and RF inputs. The two beams were combined at the mixer device for the mixing detection.

The local carrier velocity, $v(x,t)$, is proportional to the bias drop along the channel, $U_{ch}(x,t)$. At the same time, the induced carrier concentration in the channel is proportional to the local gate to channel bias, $n \sim U_g(x,t) - U_{ch}(x,t)$. The induced current is given by $j(x,t) = en(x,t)v(x,t)$. Both carrier concentration and velocity are modulated by the THz frequency, $n(x,t) = n_0(x) + n_{RF}(x)\cos(\omega t)$ and $v(x,t) = v_0(x) + v_{RF}(x)\cos(\omega t)$. The product of carrier concentration and velocity has a term that is proportional to $\cos^2(\omega t)$. This provides a DC term since $\cos^2(\omega t) = 0.5 + 0.5\cos(2\omega t)$. The resulting local rectified bias is given by

$$dU(x) = \frac{2U_G^{LO}(x)U_{ch}^{RF}(x)\cos\varphi - \left(U_{ch}^{RF}(x)\right)^2}{4(U_G^{DC} - U_{ch}^{DC})} e^{i\xi(x)} dx/L \qquad (eq.1)$$

, where φ is the relative phase between the THz biases applied between drain and source ($U_{ch}^{RF}(x)$ and $U_G^{LO}(x)$). $\zeta(x)$ takes a phase shift of the created bias due to the spreading plasma wave into account. The total bias generated by the device can be obtained by integrating (eq.1). For transistors operating below the transit time cut off frequency, the phase $\zeta(x) \approx$ const and the integration is simply the sum over all local

biases. The local biases can then be substituted by the total bias drops along the channel, U_{ch}^{RF}, and gate, U_G^{LO}, resulting in a total THz induced DC bias of

$$U_r \approx \frac{2U_G^{LO} U_{ch}^{RF} \cos\varphi - \left(U_{ch}^{RF}\right)^2}{4(U_G^{DC} - U_{ch}^{DC})} \qquad (eq.2)$$

The device behaves like a lumped element transistor due to negligible phase shifts along the channel. Above the cut-off frequency however, the spreading plasma wave induces phase shifts such that a lumped element approach is generally not valid. For THz rectifying transistors it turns out that the THz fields decay sufficiently fast on timescales (much) shorter than the transit time of the carriers (transistors operating above the transit time cut off frequency). Therefore, a quasi-static description by a (eq.2) remains valid for FETs operating at THz region. We can rewrite (eq.2) in terms of radiation power as follows,

$$U_r \approx \frac{2R\sqrt{P_G^{LO} P_{ch}^{RF}} \cos\varphi - R P_{ch}^{RF}}{4(U_G^{DC} - U_{ch}^{DC})} \qquad (eq.3),$$

where R is the antenna impedance *and* $P=U^2/R$ is the radiation power.

The first term in (eq.3) is proportional to the square-root of product of LO and RF power, and describes the multiplicatively mixed signal (ex. for constant P_G^{LO}, the detected signal is proportional to $\sqrt{P_{ch}^{RF}}$). We note that there is no term proportional to $(P_G^{LO})^2$, which can become a very large background DC signal. However, the LO signal applied to the gate can leak to the channel as $P_{ch}^{tot}=P_{ch}^{RF}+\beta P_G^{LO}$, and therefore can lead to direct detection of LO power. Accordingly, (eq.3) may be modified as

$$U_r \approx \frac{2R\sqrt{P_G^{LO}(P_{ch}^{RF} + \beta P_G^{LO})} \cos\varphi - R\left(P_{ch}^{RF} + \beta P_G^{LO}\right)}{4(U_G^{DC} - U_{ch}^{DC})} \qquad (eq.4)$$

The sign and the magnitude of β depend on the device layout and local resistances between gate-source and drain-gate.

Experimentally, $\beta=0$ could be achieved by appropriate biasing and the choice of a symmetric device structure. The multiplicatively mixed signal (first term in (eq.3)) can be detected by modulating the LO beam with a chopping blade (the second term in (eq.3) is filtered out). The resulting output signal is purely due to the multiplicative mixing, therefore is proportional to the square-root of the input THz power ($V_{out} \sim \sqrt{P_{ch}^{RF}}$) as in the green data in Figure 8 and the black data in Figure 10. The second term of (eq.3) can be detected by turning off the LO source. The resulting output signal is linearly proportional to the input THz power ($V_{out} \sim P_{ch}^{RF}$) as in the black data in Figure 8 and the red data in Figure 10.

4.2 Fabrication

Accordingly, we fabricated FET multiplicative mixers with two crossed dipole antennas for the two input channels (LO and RF channels) as illustrated in Figure 6.
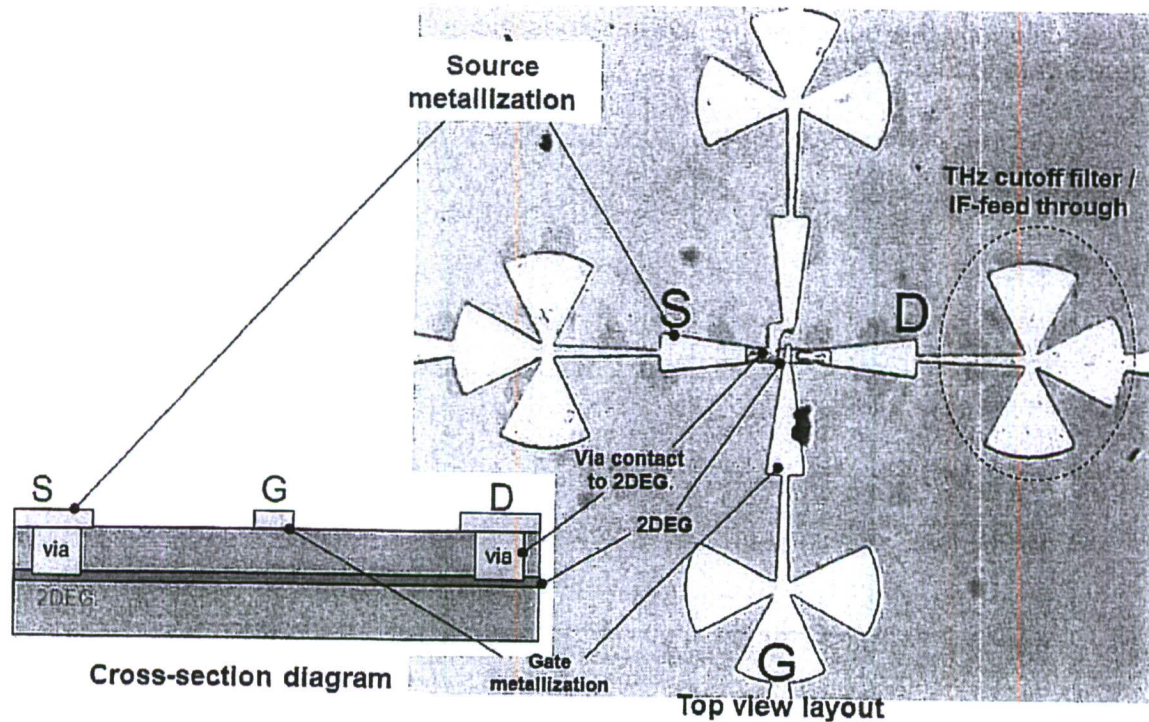
Figure 6: (left) cross-sectional diagram and (right) top-view micrograph of the fabricated device.

4.2.1 Details of the fabrication process

The following processing procedure was used to develop a set of FET mixer devices on 2-inch diameter AlGaAs-based 2DEG sample wafers.

  a) 2-dimensional electron gas (2DEG) samples were grown (Professor Arthur Gossard's laboratory at the UCSB Materials Department).
  b) Source and drain areas were defined with contact lithography.
  c) Via contacts to the 2DEG were etched.
  d) Deposition of 200 nm thick metal layer to finish the fabrication step.

4.3 Test Results

The fabricated FET mixer devices were mounted on a silicon lens and were tested in a homodyne measurement system as illustrated in Figure 5. During the initial measurement efforts, we found out that our mixers did not provide sufficient sensitivity at the 670 GHz design frequency (See Section 4.4 for the discussions over the possible causes). We therefore moved to a lower illumination frequency band, and our mixers were instead characterized at the 300~400 GHz band. Our THz sources (frequency-multiplied souces at UCSB) provided 10~20 dB higher output power in the lower frequency band and the fabricated antenna-filter structure provided strong resonant coupling at this lower band (Figure 4).

As a result, we could measure non-zero output signals that are consistent with the expected homodyne mixing system; the output signal oscillates as the optical path length of one of the two beams is adjusted with a delay stage (See Figure 5 and Figure

7). Additionally the output signal increases as the square-root of the input THz power (green data in Figure 8).
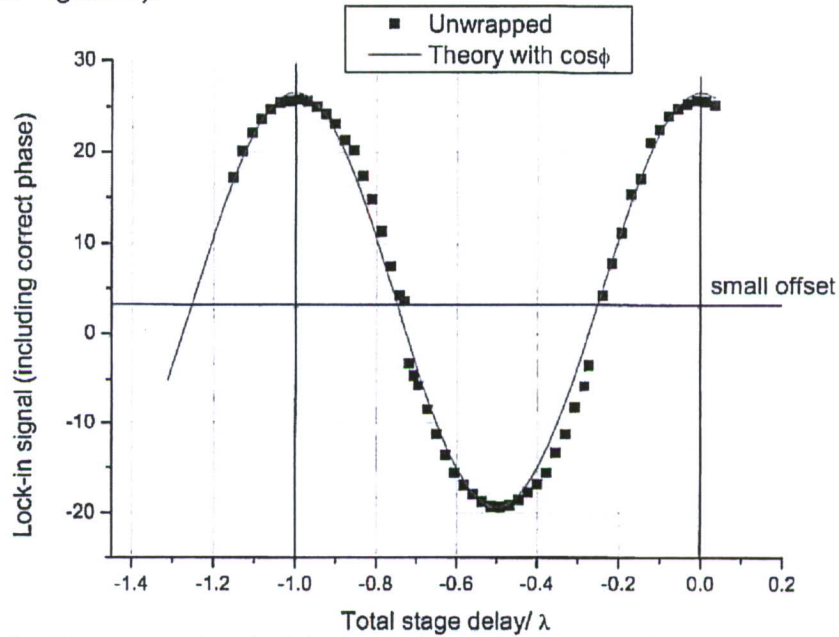

Figure 7: The output signal of the homodyne mixer system (Figure 5) oscillates as the delay of the beam line (beam ① in Figure 5) is adjusted. The small offset is due to the leakage (or cross-talks) of the crossed antenna system.
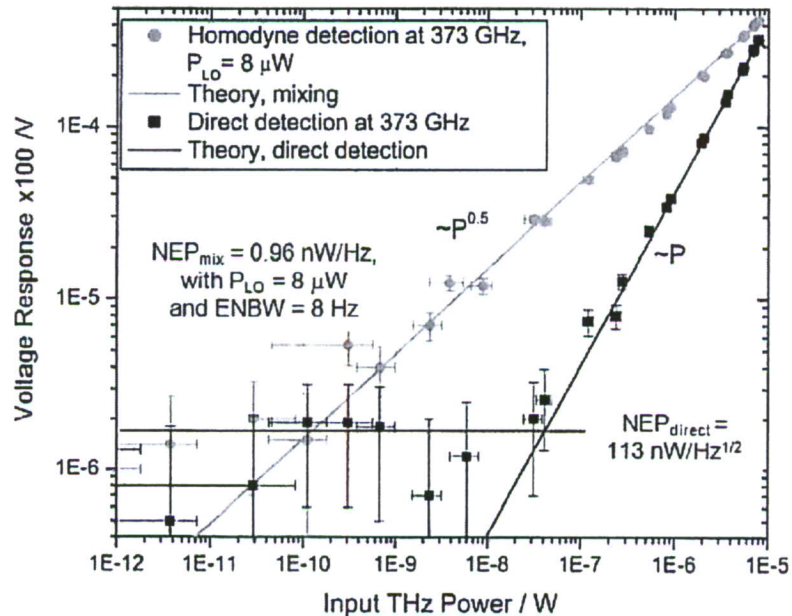

Figure 8: Measured detector responses vs. input THz power at 373 GHz in homodyne mixing (green) and direct (black) detection modes. In this log-log plot, the slope of 0.5 indicates mixing detection, whereas the slope of 1 indicates direct detection. The homodyne mixing mode resulted in noise equivalent power of 1 nW/Hz with LO power (P_{LO}) of 8 μW. The input THz power was calibrated with a power meter [3] and was varied with rotating wire grid polarizers as illustrated in Figure 5.

In order to estimate a noise equivalent power (NEP), the terahertz input power (output power of our THz source measured at the position of our mixer) was calibrated with a terahertz power meter [3]. From the minimum input THz power which achieves signal to noise of 1 (input THz power at the cross point of the noise floor and the mixer response line in Figure 8), the NEP of the first generation of our devices was estimated to be 1 nW/Hz. This NEP was 54 dB higher than the NEP of state-of-the-art Schottky diode mixer heterodyne receivers (3.9 fW/Hz [4]). However, our mixers used a 21 dB lower local oscillator power (P_{LO}) of 8 μW, compared to the 1 mW P_{LO} used for the determination of the Schottky diode mixers [5]. Since the NEP is known to scale as the inverse of P_{LO} ($NEP \sim 1/P_{LO}$ [6]), our device has a performance that is only **33 dB worse than the performance of the SOA Schottky diode mixers (assuming they are tested with the same P_{LO})**. The above results were obtained from the first generation devices and we believed there to be significant room for improvements in that initial design. As discussed in the next sections, the multiplicative FET mixers can improve greatly if key problem areas were properly addressed.

4.4 What we have learned from the first generation of devices at 370 GHz

The test results indicate some flaws in the design of the first generation devices. Firstly, we measured very high contact resistances (~9 kΩ), which would be expected to result in a lower-than-expected responsivity, by dissipating a large portion of the input THz power. Contact resistance can be lowered to a few Ohms by refining the fabrication processing techniques. Secondly, we observed a high level of noise. We think that the noise floor of our current experimental setup is swamped by 1/f noise due to the slow modulation frequency of ~50 Hz modulator that was used in the test setup. Higher chopping frequencies, near 1 kHz, would be expected to reduce the measured noise in the test setup. The 1/f noise may be further reduced in the future with high IF-frequency (e.g., MHz) heterodyne mixing scheme. Thirdly, we observed significant cross-talks between the two orthogonal antennas under certain bias conditions. The cross-talks can raise the background noise level and reduce the dynamic range of the mixer. We found a way to minimize the cross-talks with proper bias voltages (effectively isolating the two antennas). In the future, the cross-talks may be suppressed with a high quality insulation layer that separates the two antennas (e.g., SiO_2 layer of Si MOSFET architecture). Lastly, considering the channel resistance around 1kΩ, an anti-resonant dipole antenna ($Z_{ant} \sim 300$ Ω, antenna length $\sim \lambda$) would be better for impedance-matching than a resonant dipole antenna ($Z_{ant} \sim 10$ Ω, antenna length $\sim \lambda/2$) (see Figure 3).

If these problems are properly addressed, we estimate that our FET mixers would achieve a NEP of <fW/Hz with a P_{LO} of ~1 μW (a theory paper [2] will be published soon). This argument is supported by similar research done by a German group [7], which demonstrated a NEP of 8 fW/Hz with a P_{LO} of 2 μW with Si MOSFETs and with a slightly different mixing scheme (additive mixing). Their research suggests that FET-based mixers can out-perform the diode-based mixers by at least 30 dB.

These results and analyses strongly suggest that a significant impact and improvement in the design of THz systems could be achieved. For example, a diode mixer requires P_{LO} of 1 mW, and therefore, a 100x100 array of mixers would require 10,000 local oscillators integrated on a chip. This is not readily achievable with current

SOA technologies [8], nor is the dissipation of 10 W (= 10,000 x 1 mW) of power on a single chip easily handled. In contrast, FET-based mixers would require smaller P_{LO} (e.g., 1 µW) to achieve the same signal to noise ratio (SNR). A single 10 mW LO source can be employed to quasi-optically illuminate the whole 100x100 pixel array [7]. Each pixel would receive the required P_{LO} of 1 µW. FET-based mixers can be the enabling technology for the low-cost THz focal plane array imager.

4.5 Second generation of devices at 570 GHz

We renewed our project goals in the second portion of the funded effort to develop improved performance of our multiplicative mixers. As a result, the second generation mixers achieved a demonstrated operating frequency of up to 570 GHz.

We tried to implement as many of the improvement strategies (Section 4.4) as possible with our currently available resources. An initial attempt to improve the contact resistance by increasing VIA contact area was not successful; though a somewhat lower resistance (6.2 kΩ instead of previous 9 kΩ) was obtained, NEP did not improve. As an additional attempt to lower the resistance further, we fabricated mixers out of InGaAs samples (higher mobility than previous AlGaAs). This reduced the channel resistance to 2 kΩ and helped raise the operating frequency to 570 GHz. The modulation chopping frequency unfortunately could not be increased higher than 50 Hz in the available test setup, due to the limitation of the large custom-made mechanical chopper blade. A fast electronic switch (such as PIN diode) was also not available within the time frame of the tests. We were able to perform fine adjustments to the bias conditions on the devices under test, to achieve minimal cross-talk between the antennas. This was not successful in reducing NEP, due to the fact that any non-zero bias would add significant noise to the system. Finally we were able to add to the mixer design, anti-resonating antenna patterns for 570 GHz for better impedance-matching with kΩ-level channel resistance.
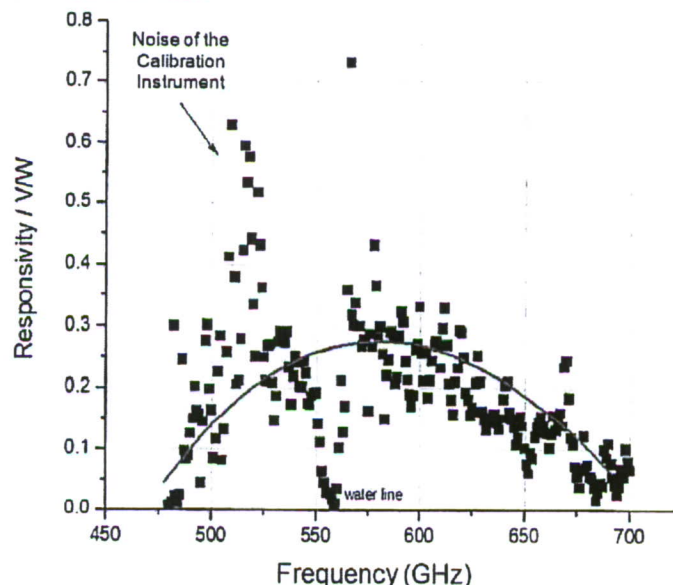

Figure 9: mixer signal responsivity (V/W) vs. frequency (GHz) of the second generation of devices at 570 GHz band. In comparison, 1st generation data at 370 GHz is shown in Figure 4.

Thanks to the reduced channel resistance and better antennas at 570 GHz, the second generation of mixers demonstrated some improvement in NEP and operated at a higher frequency (at 570 GHz, see Figure 9) than the previous first generation devices (at 370 GHz, see Figure 4).

In the revised wafer layout designs, we also fabricated devices designed for operation at 370 GHz, for the purpose of comparing against the first generation of fabricated devices at 370 GHz. However, due to the poor yield of the AlGaAs devices, there was no working 370 GHz devices produced in the second generation fabrication, making it difficult to estimate how much improvement we made over the first generation of devices. The improvements achieved with the second generation mixer design may only be inferred from the increase in the operating frequency response from 370 GHz to 570 GHz. The measured *NEP* for the second generation of devices was 26.4 nW/Hz with P_{LO} of 1.5 µW (see Figure 10).
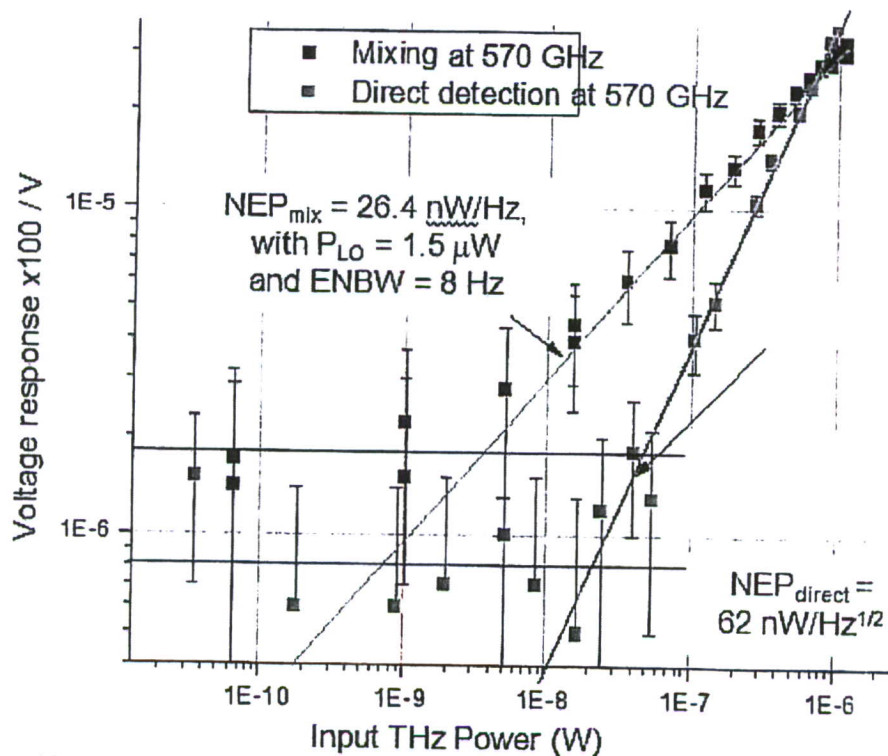

Figure 10: measured mixer signal voltage (x100 V) vs. input THz power (W) at 570 GHz in homodyne mixing (black) and direct (red) detection modes. The homodyne mixing mode resulted in noise equivalent power of 26.4 nW/Hz with LO power (P_{LO}) of 1.5 µW. In comparison, 1st generation data at 370 GHz is shown in Figure 8.

5 Current status and beyond

We have achieved the critical goal (a proof of concept demonstration) of this modified Phase II STTR project. We have fabricated the FET multiplicative mixers using a contact lithography process on AlGaAs (1st gen.) and InGaAs (2nd gen.) samples, and tested the fabricated mixers with a homodyne detection system. Based on the initial experimental results (1st gen.), we suggested a roadmap to improve the performance of these devices, and demonstrated an improvement (in terms of higher

operating frequency) by implementing lower resistances and better antennas in the 2nd generation designs. Two journal papers ([1] and [2]) have been submitted for publication.

For the continuation of this effort beyond this modified phase II STTR project, Tanner is actively building a partnership with a system integrator company (SAIC; http://www.saic.com). SAIC and Tanner are currently working together to develop a program for a low cost THz focal plane array imager for real-time standoff screening of hidden weapons in a military context [9].

6 References:

[1] S. Preu, S. Kim, R. Verma, P. G. Burke, N. Q. Vinh, M. S. Sherwin, and A. C. Gossard, "Terahertz detection by a homodyne field effect transistor multiplicative mixer," submitted to the Applied Physics Letters on June 29, 2011. (recently turned down. We will submit it to another journal)

[2] S. Preu, S. Kim, R. Verma, P. G. Burke, M. S. Sherwin, and A. C. Gossard, "An improved theory for non-resonant THz detection in field-effect-transistors," Submitted to the Journal of Applied Physics on July 14, 2011.

[3] Absolute terahertz power-energy meters by Thomas Keating, Inc. http://www.terahertz.co.uk/index.php?option=com_content&view=article&id=140&Itemid =443.

[4] Peter H. Siegel and Robert J. Dengler, "TERAHERTZ HETERODYNE IMAGING PART I: INTRODUCTION AND TECHNIQUES," *International Journal of Infrared and Millimeter Waves* 27, no. 4 (January 2007): 465-480.

[5] H Roser et al., "Nanostructure GaAS Schottky diodes for far-infrared heterodyne receivers," *Infrared Physics & Technology* 35, no. 2-3 (March 1994): 451-462.

[6] E. R. Brown, "Fundamentals of terrestrial millimeter-wave and THz Remote Sensing," in *Terahertz Sensing Technology Volume II: Emerging Scientific Applications and Novel Device Concepts*, D. L. Woolard, W. R. Loerop, and M. S. Shur, Eds, Singapore: World Sci., 2003.

[7] Diana Glaab et al., "Terahertz heterodyne detection with silicon field-effect transistors," *Applied Physics Letters* 96, no. 4 (2010): 042106.

[8] Imran Mehdi et al., "Radiometer-on-a-chip: a path toward super-compact submillimeter-wave imaging arrays" (presented at the Terahertz Physics, Devices, and Systems IV: Advanced Applications in Industry and Defense, Orlando, Florida, USA, 2010), 767105-767105-9, http://link.aip.org/link/PSISDG/v7671/i1/p767105/s1&Agg=doi.

[9] The team submitted a proposal in response to the National Small Arms Center (NSAC) FY12 request for project proposal.